Article

Ultralow-Fouling Behavior of Biorecognition Coatings Based on Carboxy-Functional Brushes of Zwitterionic Homo- and Co-polymers in Blood Plasma: Functionalization Matters

Hana Lísalová, Eduard Brynda, Milan Houska, Ivana Víšová, Kate#ina Mrkvová, Xue Chadtová Song, Erika Gedeonová, František Surman, Tomáš Riedel, Ognen Pop-Georgievski, and Jiri Homola

Anal. Chem., **Just Accepted Manuscript** • DOI: 10.1021/acs.analchem.6b04731 • Publication Date (Web): 24 Feb 2017

Ultralow-Fouling Behavior of Biorecognition Coatings Based on Carboxy-Functional Brushes of Zwitterionic Homo- and Co-polymers in Blood Plasma: Functionalization Matters

Hana Lísalová[1], Eduard Brynda[2], Milan Houska[2], Ivana Víšová[1], Kateřina Mrkvová[1], Xue Chadtová Song[1], Erika Gedeonová[1], František Surman[2], Tomáš Riedel[2], Ognen Pop-Georgievski[2], and Jiří Homola[1]*

[1] Institute of Photonics and Electronics of the CAS, Chaberská 57, Prague, 182 51, Czech Republic

[2] Institute of Macromolecular Chemistry of the CAS, Heyrovského nám. 2, Prague, 162 00, Czech Republic

Prof. Jiří Homola, Ph.D., DSc., Institute of Photonics and Electronics, Czech Academy of Sciences, Chaberská 57, 18251 Prague, Czech Republic; Tel.: +420 266773404, E-mail: homola@ufe.cz

ABSTRACT: Fouling from complex biological fluids such as blood plasma to biorecognition element (BRE)-functionalized coatings hampers the use of affinity biosensor technologies in medical diagnostics. Here we report the effects the molecular mechanisms involved in functionalization of low-fouling carboxy-functional coatings have on the BRE capacity and resistance to fouling from blood plasma. The specific mechanisms of EDC/NHS activation of carboxy-groups, BREs' attachment, and deactivation of residual activated groups on recently developed ultralow-fouling carboxybetaine polymer and copolymer brushes (pCB) as well as conventional carboxy-terminated oligo(ethylene glycol)-based alkanethiolate self-assembled monolayers (OEG-SAMs) are studied using the PM-IRRAS, XPS, and SPR methods. It is shown that the fouling resistance of BRE-functionalized pCB coatings is strongly influenced by a deactivation method affecting the ultralow-fouling molecular structure of the brush and the surface charges. It is revealed that, in contrast to free carboxy-group-terminated OEG-SAMs, only a partial deactivation of EDC/NHS-activated zwitterionic carboxy-groups by spontaneous hydrolysis is possible in the pCB brushes. The fouling resistance of activated/BRE-functionalized pCB is shown to be recovered only by covalent attachment of amino acid deactivation agents to residual activated carboxy-groups of pCB. The developed deactivation procedure is further combined with ultralow-fouling brushes of random copolymer carboxybetaine methacrylamide (CBMAA) and *N*-(2-hydroxypropyl) methacrylamide (HPMAA) with optimized CBMAA content (15%) providing a BRE-functionalized coating with superior fouling resistance over various carboxy-functional low-fouling coatings including homopolymer pCB brushes and OEG-SAMs. The biorecognition capabilities of pHPMAA-CBMAA(15%) are demonstrated via the sensitive label-free detection of a microRNA cancer biomarker (miR-16) in blood plasma.

1. Introduction

Recent advances in optical affinity biosensors have increased their potential for applications in areas, such as medical diagnostics, environmental monitoring, food safety, and security [1,2]. Label-free plasmonic biosensors allow for the direct, real-time observation of interactions among biomolecules and, in contrast to commonly used label-based methods, such as enzyme-linked immunosorbent assays (ELISA) or fluorescence biosensors, do not require the use of additional reagents (*e.g.* secondary antibodies). Despite these advantages, label-free biosensors cannot discriminate between the binding of target analytes to biorecognition elements (BREs) immobilized on the sensor surface and deposition of non-target species (*i.e.* "fouling") from the tested medium [3]. This fouling may be severe from complex biological media, such as blood plasma or serum and can limit biosensor performance and increase the probability of false positive results [3,4].

Various approaches have been proposed to suppress the effects of fouling from complex samples on performance of label-free biosensors. These approaches are based on the use of reference channels or reduction of the fouling by means of surfactants. However, none of these approaches provides perfect compensation for fouling from complex biological fluids [3, 5-8]. For instance, in a typical reference-compensated approach, a reference channel is functionalized with a similar (but non-target) BRE, both the reference and detection channels are

exposed to the same sample and the sensor response in the reference channel is subtracted from that of the detection channel [3,5]. However, it is often difficult to identify BREs yielding a reference channel with fouling properties that are close to those of the sensing channel. Alternatively, both the reference and detection channels are functionalized with the same BREs and the reference channel is exposed to a reference sample, which does not contain a target analyte (*e.g.*, blood plasma obtained from healthy donors or pooled plasma). However, complex biological samples, such as blood plasma samples obtained from different people exhibit different levels of fouling [6] which may introduce a bias into the reference-compensated biosensing. In addition to the referencing approaches, various surfactants (*e.g.,* Tween) and protein-based additives (*e.g.,* serum albumin or casein) are commonly used to reduce fouling. However, their use has been shown to negatively affect the biorecognition activity of immobilized BREs [8].

Therefore, there is an intensive search for functional coatings that effectively resist plasma fouling as well as provide a sufficient amount of functional groups suitable for attachment of BREs. Although there is a variety of anti-fouling materials, *e.g.*, poly(ethylene glycol) (PEG) and its derivatives, only a few have been demonstrated as functionalized coatings for biosensing in complex media [4,5,9,10-14]. Currently, carboxy-functional brushes based on zwitterionic carboxybetaine polymers (pCB) provide the best biorecognition platforms for biosensing in complex biological fluids [4,5,10-15]. For example, poly(carboxybetaine acrylamide) (pCBAA) brushes have been demonstrated to provide superior fouling resistance from blood plasma or serum combined with a relatively high BRE capacity when compared to the widely used carboxy-functional low-fouling ω-oligo(ethylene glycol)-based alkanethiolate self-assembled monolayers (OEG-SAMs) [5,11,16]. Compared to hydroxy-functional coatings, the activation of the carboxy groups to form the active ester intermediates can be accomplished under mild conditions in a timely manner using protein-compatible water-based solvents [17,18].

The pCB functionalization consists in the transformation of carboxy groups in zwitterionic carboxybetaine side chains (CB) of the polymers to active esters, to which BREs are subsequently covalently coupled via their amine groups. The first step is usually based on *N*-ethyl-*N*'-(3-diethylaminopropyl) carbodiimide (EDC) and *N*-hydroxysuccinimide (NHS) coupling (Figure S1 in Supporting Information) [19,20]. Although the EDC/NHS activation is routinely used in numerous biosensor and bioconjugate techniques [17,21], the reaction scheme is quite complex and the reaction pathways are influenced by various reaction conditions, including reagent concentrations, incubation times, buffer composition, and the functional coating type [22-25]. According to the established reaction scheme, active esters (*i.e.*, NHS-ester or *O*-acylurea) spontaneously hydrolyze back to carboxy groups in aqueous solutions [23,24,26]. The same mechanism, *i.e.*, the spontaneous hydrolysis of all activated carboxy groups remaining in pCB after the EDC/NHS activation/attachment of BREs was supposed to recover the original ultralow-fouling structure of the pCB brushes. However, remarkable increase in plasma fouling (beyond the ultra-low fouling threshold set as 5 ng/cm^2) [11,16] was observed for pCB brushes after their activation with EDC/NHS, covalent attachment of BREs and hydrolysis-based deactivation [8,19,27] as well as upon only the EDC/NHS activation and hydrolysis-based deactivation without attachment of any BREs [8]. A similar trend but in a much higher extend was observed for hydroxy-functional brushes upon activation of their functional groups [8]. It is evident that the functionalization processes affect the fouling resistance of functionalized brushes. However, the nature of these effects is not completely understood.

In this work, to our best knowledge, it is the first time when the molecular functionalization processes with respect to both the BRE immobilization capacity and resistance to fouling from blood plasma are investigated. Specifically, the functionalization processes and their relationship with physico-chemical properties (surface charge, chemical composition) are studied on the ultralow-fouling pCB brushes and recently synthesized ultralow-fouling brushes composed of randomly arranged carboxybetaine methacrylamide (CBMAA) and *N*-(2-hydroxypropyl) methacrylamide (HPMAA) monomer units, (pHPMAA-CBMAA) [20,28] using surface plasmon resonance (SPR), polarization modulation infrared reflection/absorption spectroscopy (PM-IRRAS), and X-ray photoelectron spectroscopy (XPS). Results of this study are compared to those obtained on traditional carboxy-functional OEG-SAMs. The studied functionalization processes include EDC/NHS activation, BRE (antibody, amino-modified oligonucleotide probe) attachment, and subsequent deactivation of residual activated carboxy groups. The findings are applied in functionalization of pHPMAA-CBMAA containing an optimized molar content of CBMAA (15%) to characterize its biorecognition capabilities with respect to label-free detection of microRNA (miR-16), a biomarker of various human malignant and cardiovascular diseases [29-31], in blood plasma.

2. Experimental Section

Reagents: *N*-hydroxysuccinimide (NHS) and N-ethyl-N'-(3-diethylaminopropyl)carbodiimide (EDC) were purchased from PharmaTech, Czech Republic. Ethanol (purity ≥ 99.9%) was purchased from Merck, Czech Republic. Tris (hydroxylmethyl) aminomethane, ethanolamine (EA), imidazole, dextran sulfate (MW ~8 kDa, DS), NaCl, glycine, streptavidin, *N*-hydroxysulfosuccinimide sodium salt (sulfo-NHS), ethylenediaminetetraacetic acid (EDTA), γ-aminobutyric acid (99%), β-alanine (99%), sodium dodecyl sulfate (SDS), MgCl2, CuBr, CuBr2, 2,2'-dipyridyl (BiPy), 1,4,8,11-tetramethyl-1,4,8,11-tetraazacyclotetradecane (Me4Cyclam, 98%), CuCl (≥ 99.995%), CuCl2 (99.999%), and stock solutions for the preparation of phosphate buffered saline (PBS, 0.01 M phosphate, 0.138 M sodium chloride, 0.0027 M potassium chloride, pH 7.4 at 25 °C), 10 mM sodium borate, pH 8 (SB) at 25°C, and 10 mM sodium acetate buffer, pH 5.0 (SA) at 25 °C were purchased from Sigma-Aldrich, Czech Republic. The buffer solutions were prepared using Milli-Q water (18.0 MΩ.cm, Milli-Q). The (2-aminoethoxy)acetic

acid and [2-(2-aminoethoxy)ethoxy] acetic acid were purchased from Iris Biotech, Germany. The alkanethiols HS-$(CH_2)_{11}$-$(EG)_6$-OCH_2-COOH and HS-$(CH_2)_{11}$-$(EG)_4$-OH were purchased from Prochimia, Poland. Tetrahydrofuran (THF, purity ≥99.9%) was purchased from Penta, Czech Republic. The amino-modified DNA oligonucleotide probe, 22-mer, NH_2-$(CH_2)_{12}$-5'- CGC CAA TAT TTA CGT GCT GCT A -3' (NH_2-ON-probe), the probe functionalized with attached biotin (biotin-ON-probe), and miR-16 target (5'-r(UAG CAG CAC GUA AAU AUU GGC G) -3') were purchased as HPLC-purified from Integrated DNA Technologies, USA. The antibodies (Ab), i.e. anti-*E.coli* O157:H7 (anti-*E.coli*) and anti-*Salmonella* were purchased from KPL Inc., USA. The human blood plasma (pooled, mixed gender) in sodium citrate was donated by the Institute of Hematology and Blood Transfusion, Czech Republic. All of the tested individuals agreed to this study at the time of blood collection. The study was approved by the Institute of Hematology and Blood Transfusion Ethics Committee and all samples were obtained in accordance with the Ethical Commission's regulations and with a release of informed consent. The initiator ω-mercaptoundecylbromoisobutyrate was synthesized as described previously [32]. The monomers 3-methacryloylaminopropyl-2-carboxyethyl-dimethylammonium betaine (carboxybetaine methacrylamide, CBMAA) and *N*-(2-hydroxypropyl) methacrylamide (HPMAA) were synthesized according to the literature [33-34].

Preparation of functional coatings: The brushes of pHPMAA, pCBMAA, pCBAA, and copolymer pHPMAA-CBMAA (Scheme 1) having the thickness of ~25 nm (as measured by optical ellipsometry) were grafted from gold-coated substrates (SPR chip or Si wafer) by surface-initiated atom transfer radical polymerization (SI ATRP) as described elsewhere [20], for details, see Supporting Information. The molar percentage of CBMAA monomer units x = 7.5, 15, and 30 mol% in pHPMAA-CBMAA(x%) brushes corresponded with the molar ratios of CBMAA / (CBMAA+HPMAA) monomers in polymerization solution indicating that the CBMAA monomer units were randomly distributed in the copolymer chains. The self-assembled monolayers of HS-C_{11}-EG_6-OCH_2-COOH (COO-OEG-SAMs) and mixed HS-C_{11}-$(EG)_6$-OCH_2-COOH and HS-C_{11}-$(EG)_4$-OH, 3:7 (mixed OEG-SAMs) were prepared on gold-coated chips according to the procedure described in [8], see also Supporting Information.

Scheme 1. Chemical structures of polymer brushes used in this work. pHPMAA: poly(*N*-(2-hydroxypropyl) methacrylamide), pCBMAA: poly(carboxybetaine methacrylamide), pHPMAA-CBMAA(x%): random copolymer of HPMAA and CBMAA, where x% is the molar percentage of CBMAA monomer units in the copolymer.

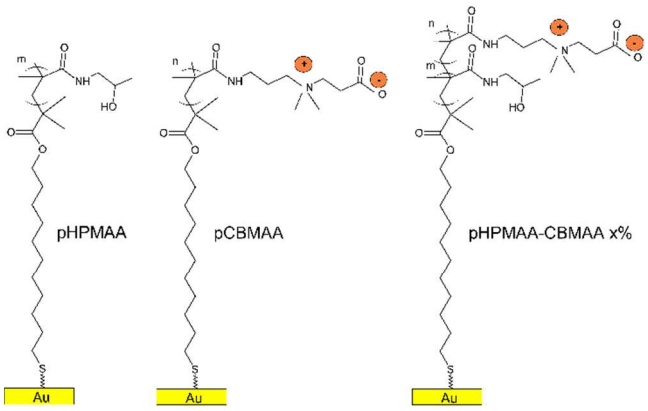

PM-IRRAS measurements: The pCBMAA and pHPMAA-CBMAA(15%) coatings formed on SPR chips were analyzed by PM IRRAS (NICOLET 6700 spectrometer with photoelastic modulation (PEM) module, Thermo Scientific, USA). The laser beam was modulated by ZnSe grid polarizer and ZnSe photoelastic modulator (HINDS Instruments, PEM 90, modulation frequency = 37 kHz) and focused on the sample at an incident angle of 82°. The reflected light was collected by a nitrogen-cooled Mercury–Cadmium–Telluride (MCT) detector. The spectra were obtained from co-addition of 100 scans with a resolution of 4 cm^{-1}. A total of four chips for each brush type were washed with Milli-Q water and dried with a stream of nitrogen and immediately mounted to the PEM module of the spectrometer. The coatings were subsequently activated with a solution of 0.1 M NHS / 0.5 M EDC + 10 mM NaCl (30 min), washed with Milli-Q water and dried with nitrogen. The infrared spectrum of a coated SPR chip was recorded immediately after the activation, whereas the other three chips were deactivated by immersion into a solution of (1) 10 mM sodium borate + 10 mM imidazole + 10 mM NaCl, pH 8.0 (D-buffer, 30 min), (2) 1 M glycine, pH 7.0 (30 min), and (3) 1 M EA, pH 8.0 (30 min) as described below.

XPS measurements: The XPS measurements were performed using a K-Alpha+ XPS spectrometer (ThermoFisher Scientific, UK) operating at a base pressure of 1.0×10^{-7} Pa. The data acquisition and processing were performed using Thermo Avantage software. All surfaces were analyzed using microfocused, monochromated Al Kα X-ray radiation (400 μm spot size) with a pass energy of 200 eV for survey and 50 eV for high-energy resolution core level spectra. The X-ray angle of incidence was 30° and the emission angle was normal to the surface. The K-Alpha charge dual compensation system was employed during analysis, using electrons and low-energy argon ions to prevent any localized charge build-up. The high resolution spectra were fitted/deconvoluted with Voigt profiles. All spectra were referenced to the C 1s peak attributed to C—C, C—H at 285.0 eV binding energy, which was controlled by means of the photoelectron peaks of poly(ethylene terephthalate) and metallic Cu, Ag, and Au.

Spectral ellipsometry measurements: Polymer brushes were grafted from gold surface of plates cut from a polished silicon wafer coated with an optically thick (100 nm) gold layer. The refractive index and thickness of the dried brush were measured on at least three spots per a plate using a spectral

ellipsometer SE 850 Sentech, Germany. For each experiment, the brushes were prepared on three gold-coated silicon plates in one batch together with gold coated plates for SPR measurements. The dry thicknesses of the brushes were in the range of 22 nm – 28 nm.

SPR measurements: A four-channel SPR sensor combined with a near-dispersionless microfluidic system [35] developed at the Institute of Photonics and Electronics (Prague, Czech Republic) was used. More details about SPR measurements are provided in Supporting Information.

3. Results and Discussion

3.1 Effect of the surface content of carboxy groups in pCB brush on plasma fouling and BRE immobilization

We investigated the effect of the relative surface content of carboxy groups in pCB brush on the antibody (Ab) immobilization capacity and fouling from full blood plasma for pHPMAA-CBMAA(*x*%) brushes (where *x* denotes mol% of CBMAA). Table 1 shows the antibody (Ab, anti-*Salmonella*) immobilization capacity, *i.e.* the maximum amount of bound Ab that can be immobilized on the coating under the given experimental conditions (column A) in comparison to homopolymer brushes of pCBMAA. Ab immobilization capacity of pHPMAA-CBMAA(*x*%) brushes pertaining to x = 15 and 30 reached ~45% and ~80% of the capacity of pCBMAA, respectively (see also Figure 1). These results show that the ratio of the number of CB groups capable of Ab coupling to the total number of CB groups contained in the brush increased with decreasing CBMAA content in the polymer. This trend can be partially attributed to a high density of CB in the surface region of pCBMAA brush where CB groups overlapped with an immobilized antibody cannot bind other antibodies. However, this trend can be also associated with the reactivity of ionized carboxy groups to EDC/NHS. Specifically, the PM-IRRAS revealed that while only 22% of the ionized carboxy groups present in pCBAA (Figure S4) and 36% in pCBMAA (Figure 2) were converted to active esters, this ratio increased remarkably (to 90%) in pHPMAA-CBMAA(15%) (Figure S3). The results indicate that the incorporation of CBMAA in inert HPMAA polymer chain increases susceptibility of the CB carboxy groups to EDC/NHS activation.

To compare the resistance of BRE-functionalized pCB brushes to fouling from full blood plasma, the amount of immobilized Ab on each brush was adjusted to 215 ng/cm^2.This value corresponded to the maximum achievable immobilization level on pCBAA under the given experimental conditions). Furthermore, prior to this study we have measured the effect of Ab levels on the fouling resistance for the pHPMAA-CBMAA(15%) coatings. We observed that the fouling increases with an increasing Ab surface coverage up to the Ab level of ~180 ng/cm^2 and then levels off (see Figure S12 in the Supporting Information). For the Ab levels in the range of 180 – 220 ng/cm^2, no significant differences in the fouling levels were observed. The Ab level of ~215 ng/cm^2 was selected for the evaluation of the fouling resistance of pHPMAA-CBMAA coatings as variations in the Ab level around this value were expected to have smaller effect on the results. This level was successfully achieved for all brushes except for pHPMAA-CBMAA(7.5%), for which a maximum Ab level of ~20 ng/cm^2 was obtained (column B). The levels of plasma fouling on unmodified copolymers pHPMAA-CBMAA were generally lower than on pCBMAA. A very high Ab level (~450 ng/cm^2) was achieved on pCBMAA under given experimental conditions. It should be noted that such a high Ab surface coverage would not be preferable for all biosensing applications due to potential unfavorable steric effects. Compared to pCBMAA, the plasma fouling on pHPMAA-CBMAA(30%) was lower by 20%, but Ab immobilization capacity was lower only by 8%. Below 30% of CBMAA both the fouling and immobilization capacity decreased rapidly with decreasing mol% of CBMAA in the copolymer (Table 1, Figure 1). At low CBMAA contents, the decrease in fouling on unmodified copolymer brushes was faster than the decrease in the Ab immobilization capacity (Figure 1).

The attachment of Ab to EDC/NHS activated pCB followed by spontaneous hydrolysis increased plasma fouling on all the tested brushes. The fouling exhibited a similar trend as that observed for unmodified copolymer brushes, *i.e.,* fouling decreased with decreasing content of CBMAA (Table 1, Figure 1). The fouling levels on Ab-functionalized pHPMAA-CBMAA(15%) were as low as 11.6 ng/cm^2, whereby the Ab immobilization capacity was still high (~200 ng/cm^2). These levels are comparable with those reported for Ab-functionalized pCBAA in Ref. [27, 8]. On the other hand, even lower fouling values have been achieved for Ab-functionalized pCBAA [27,16]. These variations may be in a large part related to differences in composition of plasma samples used in different fouling resistance experiments [35]. Furthermore, the trend of decreasing plasma fouling with decreasing CBMAA molar content in pHPMAA-CBMAA(*x*%, *x*<60) was significantly slower for pHPMAA-CBMAA(*x*%, *x*<60) brushes functionalized with Ab and deactivated by hydrolysis compared to unmodified pHPMAA-CBMAA(*x*%) coatings. It is hypothesized that this phenomenon can be attributed to the presence of immobilized BREs as well as incomplete deactivation of activated carboxy groups in zwitterions of the pCB brush.

TABLE 1. Fouling from undiluted blood plasma on the SPR chip coated with pCB brushes. The pHPMAA-CBMAA(*x*%) brushes were functionalized by the covalent attachment of anti-*Salmonella* (Ab) to EDC/NHS-activated pCB. Column A: maximum Ab immobilization capacity, B: adjusted Ab capacity for the measurement of plasma fouling (see column D), C: plasma fouling measured on unmodified polymer brush, D: plasma fouling measured on the Ab-functionalized brush (with the Ab levels shown in Column B) and deactivated by hydrolysis.

Polymer brush	Immobilized antibody [ng/cm^2]		Fouling from blood plasma [ng/cm^2]	
	A	B	C	D
pCBMAA	450.8±28.5	208.6±13.2	11.1±2.8	25.4±4.1
pHPMAA-CBMAA(30%)	362.2±21.3	211.3±10.2	10.0±3.5	23.4±3.9
pHPMAA-CBMAA(15%)	201.6 ±10.1	201.6±11.6	2.9±0.8	11.6±2.8
pHPMAA-CBMAA(7.5%)	20.1±5.8	20.1±3.2	0.0±0.03	2.6±1.2

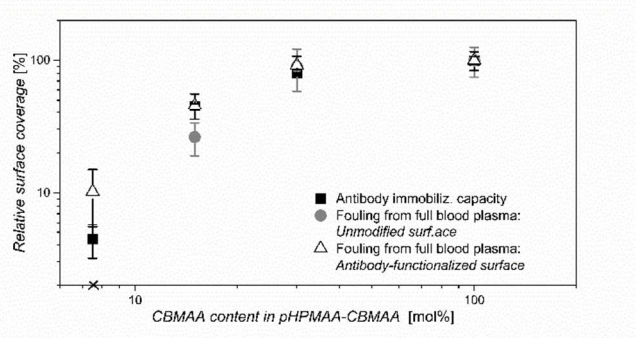

Figure 1. Antibody immobilization capacity and fouling from full blood plasma on unmodified and antibody (anti-*Salmonella*)-functionalized pHPMAA-CBMAA random copolymer brushes as a function of the relative surface molar content of CBMAA (x) in pHPMAA-CBMAA(x%). All the surface coverage values were normalized to maximum values achieved on pCBMAA (Table 1). The symbol "×" refers to the plasma fouling value achieved on unmodified pHPMAA-CBMAA(7.5%) that was below the limit of detection of the used SPR sensor.

3.2 Characterization of activation/deactivation mechanisms in pCB brushes and OEG-SAMs

The activation and subsequent deactivation of EDC/NHS-activated carboxy groups were measured by PM-IRRAS and XPS methods for pCB homopolymer and copolymer brushes as well as OEG-SAMs (Figure 1 and Figures S3-S7 in Supporting Information). Three different deactivation procedures were analyzed: deactivation by hydrolysis in deactivation buffer with optimized composition (D-buffer), deactivation with glycine, and ethanolamine (EA). Specifically for pCBMAA, the PM-IRRAS spectrum of pCBMAA brush in the dry state before activation (Figure 2, curve 1) shows the amide I band at 1650 cm^{-1} and the amide II band at 1538 cm^{-1} overlapped with the prominent band of ionized carboxy groups at 1608 cm^{-1} (asym). The ionized carboxy groups also largely contribute to the band at 1368 cm^{-1} (sym). The band 1725 cm^{-1} of non-ionized carboxy groups is rather weak; however, it suggests that not all carboxy groups are engaged in an internal interaction with quaternary ammonium cation, as it would be expected in betaines. The spectrum after EDC/NHS activation (curve 2) shows only weak bands of NHS ester at 1818 cm^{-1}, 1790 cm^{-1}, and 1735 cm^{-1} overlapped with the band of non-ionized carboxy group at 1725 cm^{-1}. The intensity of ionized carboxy group at 1608 cm^{-1} decreased markedly after the activation (down to about 60%). This indicates that either some carboxy groups engaged in a strong internal hydrogen bonding (the C=O band would shift to the region around 1660 cm^{-1} and be overlapped by a much stronger amide I band) or some other intermediates might be present. The spectra 3-5 in Figure 2 show the effects of different deactivation approaches, specifically, the deactivation of activated pCBMAA by hydrolysis of NHS ester in D-buffer (spectrum 4), and by reactions with EA (spectrum 5) and glycine (spectrum 3). The hydrolysis in optimized hydrolysis-promoted deactivation buffer (D-buffer) led to the disappearance of NHS-ester bands and decrease of the intensity of non-ionized carboxy group; however, the intensity of the band at 1608 cm^{-1} indicates a regeneration of only about 70% of the ionized carboxy groups compared to the initial pCBMAA. This observation contrasts with the assumption of spontaneous hydrolysis of NHS esters in aqueous solutions. The reaction with EA (5) does not regenerate carboxy groups (amide group is formed and hydroxy group is attached) and only 60% of ionized carboxy groups are present. The spectrum 3 after the reaction with glycine shows a rather different picture - it indicates an increase of the content of the ionized carboxy groups to 90%, apparently due to the attachment of new carboxy groups. The basic features of the spectra of pCBAA brushes (Figure S4) were rather similar to those of pCBMAA, yet the spectrum of the initial pCBAA does not show any signs of the presence of non-ionized carboxy groups. The decrease in the intensity of the band at 1608 cm^{-1} after activation (to 78%), and nearly no observable bands of NHS ester, suggest that pCBAA is less prone to the activation by EDC/NHS than pCBMAA.

Compared to activation with EDC/NHS, a much higher level of activation of carboxy groups was achieved by the reaction of pCBMAA (Figure S5) or pHPMAA-CBMAA(15%) (Figure S6) brushes with EDC/sulfo-NHS. The spectra of the activated brushes show the decrease in the intensity of the band at 1608 cm^{-1} (to 45%), the well-developed NHS ester bands at 1815 cm^{-1}, 1785 cm^{-1} and 1740 cm^{-1} (overlapped with the band 1725 cm^{-1}), and also an intense band at 1235 cm^{-1} of sulfo group in sulfo-NHS ester. The sulfo-NHS ester bands disappeared after the deactivation with EA.

The IR data are in a general agreement with the XPS measurements of sulfur present in sulfo-NHS esters bound to pCBMAA brush (Table S1). The relative content of sulfur (1.95 atomic%) in pCBMAA activated by EDC/sulfo-NHS decreased to 0.72 atomic% after incubation with D-buffer and to zero after the reaction with EA. This suggests a complete removal of sulfo-NHS ester. The relative content of sulfur (1.1 atomic%) in pHPMAA-CBMAA(15%) activated by EDC/sulfo-NHS decreased to zero after both incubation with D-buffer and after the reaction with EA.

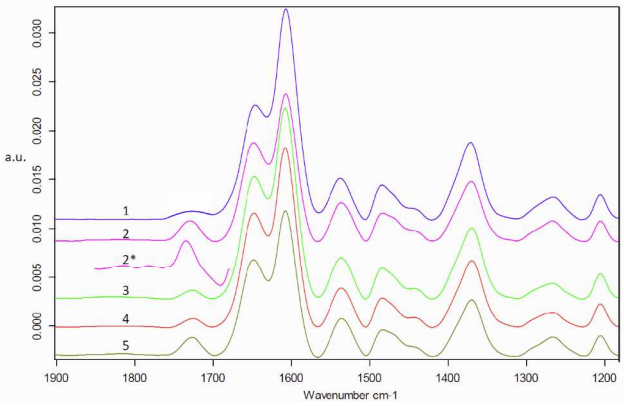

Figure 2. PM-IRRAS spectra of pCBMAA on SPR chip pertaining to the activation with EDC/NHS. 1: pCBMAA before activation; ([COO-] = 100%), 2: pCBMAA after activation with EDC/NHS; ([COO-] = 60%), 2*: difference in the spectra (2-1, expanded), 3: pCBMAA after activation and deactivation with glycine; ([COO-] = 90%), 4: pCBMAA after activation and deactivation with D-buffer; ([COO-] = 70%), 5: pCBMAA after activation and deactivation with EA; ([COO-] = 60%).

In summary, the PM-IRRAS results shown in Figure 2 and Figures S3-S6 in Supporting Information confirmed that

carboxy groups in the pCB brushes were converted to active esters. However, the PM-IRRAS measurements also revealed that carboxy groups were not fully recovered upon hydrolysis of the activated pCB brushes. A relatively low yield of hydrolysis on pCB brushes was further confirmed by XPS analysis. It should be noted, that this result is not consistent with the commonly accepted assumption of a fast and complete hydrolysis of active esters in aqueous solutions (see Figure S1). This trend was also assumed to convert all residual active esters in functionalized pCB back to carboxy groups [16,27]. On the other hand, we observed a complete hydrolysis of active esters in activated COOH-OEG-SAMs (Figure S7 and Table S1 in Supporting Information), where carboxy groups were fully recovered by incubation with D-buffer during 30 min after activation. These results suggest important differences in the reactivity of carboxy groups in CB side chains of polymer brushes and free carboxy groups, such as those on surface of low-fouling COOH-OEG-SAMs. Compared to the free carboxy groups in COOH-OEG-SAMs, a strong internal electrostatic interaction of carboxy groups with quaternary ammonium cations in zwitterionic CBs seems to make their activation by EDC/NHS and recovering by hydrolysis more difficult.

The effect of different deactivation procedures on plasma fouling in relation to surface charge was further measured for pHPMAA-CBMAA(15%) brushes after the EDC/NHS activation (Table 2). The potential changes in the net surface charge that are associated with EDC/NHS chemical processes were measured by electrostatic adsorption of a strong polyanion, dextran sulfate (DS), to activated/deactivated pHPMAA-CBMAA(15%). Table 2 shows that DS does not adsorb on pHPMAA-CBMAA(15%) before activation, indicating a net surface neutrality, even though the PM-IRRAS spectra of pCBMAA brushes measured in the dry state indicated a small portion of non-ionized carboxy groups (see Figure 2 and Supporting Information). After the activation with EDC/NHS, carboxy groups are converted to a neutral NHS-ester, resulting in a net positive charge (of quaternary ammonium cation) and an increase of DS adsorption to 77 ng/cm^2. The strong dependence of DS adsorption on the deactivation procedure is illustrated in Table 2. As expected, deactivation with EA resulting in a replacement of electroneutral NHS ester with neutral amide and hydroxy groups had only a small effect on the surface positive charge; DS adsorption was ~70 ng/cm^2. A bit smaller, but still rather high amount of adsorbed DS, 60 ng/cm^2, was observed for coatings deactivated by hydrolysis with D buffer. These results are in agreement with PM-IRRAS spectra and confirm prevailing positive charge, *i.e.*, the deficit of carboxylate anions. The most efficient deactivation procedure with respect to the compensation of the positive charge was reaction with glycine, which led to a DS adsorption of ~30 ng/cm^2. This is apparently due to the replacement of NHS esters by covalently attached glycine with negatively charged carboxy groups.

As predicted by the surface charge measurements, the lowest plasma fouling was observed on pCB brushes deactivated by the reaction with glycine. Accordingly, the PM-IRRAS and XPS results (see Figure 2 and Supporting Information) demonstrated the highest amount of regenerated carboxy groups after the deactivation with glycine. Furthermore, the same trend was observed on pHPMAA-CBMAA(15%) to which model BREs, i.e. anti-*E.coli* and NH_2-ON-probes were immobilized (Table 3). As a result, the Ab-functionalized and glycine-deactivated pHPMAA-CBMAA(15%) brush exhibited resistance to fouling from full blood plasma that was comparable to that of the state-of-art ultralow-fouling antibody-functionalized pCBAA coating with a similar Ab level. We hypothesize that a relatively low number of CBMAA monomer units randomly distributed in inert pHPMAA do not influence the formation of a well-packed brush architecture and thus helps the copolymer to attain fouling resistance similar to that of the ultra-low fouling pHPMAA.

Besides glycine, several other amino acids, varying in spacer structure and spacer length between zwitterionic amino and carboxy groups for different binding conditions, were analyzed with respect to DS adsorption and plasma fouling (see Table S2 in Supporting Information). A trend of decreasing plasma fouling with decreasing spacer length was observed. We believe that this can be attributed to a recovery of zwitterionic structure due to a closer proximity of zwitterionic groups. Accordingly, the lowest plasma fouling was observed for glycine and (2-aminoethoxy)acetic acid.

TABLE 2. Effect of different deactivation procedures on blood plasma fouling and adsorption of dextran sulfate (DS) measured on activated pHPMAA-CBMAA(15%).

pHPMAA-CBMAA(15%) functionalization step	Plasma fouling [ng/cm^2]	DS [ng/cm^2]
Before activation	4.9 ± 2.,0	0.0 ± 0.0
Activated	135.5 ± 12.6	76.5 ± 9.4
Activ./glycine-deactiv.	5.1 ± 2.6	31.1±5.4
Activ./EA-deactiv.	14.8 ± 4.9	69.7±7.3
Activ./hydrolysis-deactiv.	12.5 ± 3.1	61.2±5.5

TABLE 3. Effect of different deactivation procedures on blood plasma fouling and adsorption of dextran sulfate (DS) measured on pHPMAA-CBMAA(15%) brushes activated with EDC/NHS and functionalized (via covalent attachment) with either anti-*E.coli* or NH_2-ON-probes with densities 201 ng/cm^2 and 1.4 ×10^{13} probes/cm^2, respectively.

Deactivation procedure	Fouling from undiluted blood plasma [ng/cm^2]	
	Anti-*E.coli*-functionalized	NH_2-ON probe-functionalized
Glycine	6.6 ± 3.6	4.9 ± 2.3
EA	19.6 ± 4.5	12.4 ± 3.8
Hydrolysis	10.8 ± 2.7	13.1± 2.8

3.3 Biorecognition capabilities of functionalized pHPMAA-CBMAA(15%) in blood plasma

The biorecognition capabilities of pHPMAA-CBMAA brushes with previously optimized molar content of CBMAA (15%) [28] functionalized with DNA-ON-probes and deactivated by glycine were characterized via the direct detection of a microRNA (miR-16) in 50% blood plasma (Figure 3). The surface concentration of NH_2-ON-probes (covalently attached

to the EDC/NHS activated brush) was ~1.4×10^{13} probes/cm^2. The SPR detection experiments revealed a high degree of resistance to fouling; the fouling levels were ~2.9 ng/cm^2 and ~4.9 ng/cm^2 for 50% and full blood plasma, respectively. To the best of our knowledge, such a high fouling resistance in full blood plasma combined with a very high ON immobilization capacity has not been previously reported for any of ON-functionalized low-fouling coatings. Furthermore, the pHPMAA-CBMAA(15%) brushes functionalized with NH_2-ON-probes exhibited high biorecognition capabilities in blood plasma: the LOD for the detection of miR-16 was calculated as 6 nmol/L. This LOD is comparable to the values reported for SPR biosensors for the direct label-free detection of miRNAs in buffers [37, 38].

The biorecognition capabilities of pHPMAA-CBMAA(15%) were further compared to mixed OEG-SAMs using the same detection conditions. As it was possible to attach only a negligible amount of NH_2-ON-probes to activated carboxy groups of mixed OEG-SAMs (see Supporting Information), the mixed OEG-SAMs were functionalized with streptavidin to which biotin-ON-probes with the same DNA sequence were attached. This approach provided an ON-probe immobilization level of 4.5×10^{12} probes/cm^2 and a subsequent fouling from 50% blood plasma was ~151 ng/cm^2. This level was in a very good agreement with previously reported plasma fouling levels for antibody-functionalized unblocked mixed OEG-SAMs [8]. Conversely to the results achieved for ON-functionalized pHPMAA-CBMAA(15%), the ON-functionalized mixed OEG-SAMs did not exhibit any reasonable sensor response to miR-16 detection in 50% blood plasma, even at high analyte concentrations (see Supporting Information). Similar detection experiments for the mixed OEG-SAMs performed in buffer (without any blood plasma) showed a high biorecognition performance (see Figure S10 in Supporting Information). It can be concluded that plasma fouling on mixed OEG-SAMs led to a critical impairment of biorecognition capability of the coating.

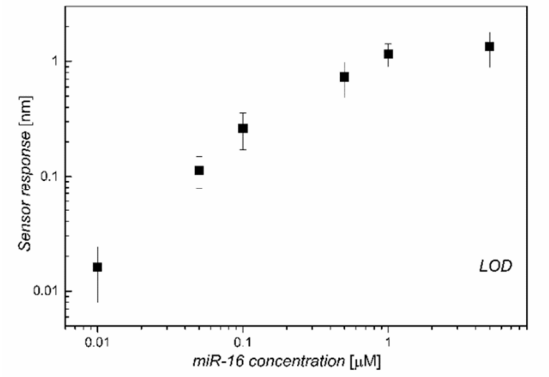

Figure 3. Sensor calibration curve for miR-16 spiked into 50% pooled blood plasma measured using pHPMAA-CBMAA(15%) brushes functionalized by covalent attachment of NH_2-ON probes.

4. Conclusions

We investigated the fundamental physico-chemical processes involved in the functionalization of carboxy-functional low-fouling coatings, including the ultralow-fouling polymer and copolymer brushes containing zwitterionic carboxybetaine side chains as well as conventional carboxy-terminated OEG-SAMs. The lowering of CBMAA content in pHPMAA-CBMAA was found to increase reactivity of carboxy groups to EDC/NHS activation, increase the ratio of BRE immobilization capacity to the total number of CB contained in the brush, and decrease the fouling from blood plasma. Furthermore, the results revealed an importance of effective deactivation of residual active esters in pCB after EDC/NHS activation and covalent coupling of BREs with regard to plasma fouling. In contrast to carboxy-terminated OEG-SAMs, the activated pCB brushes were capable of only partial deactivation of EDC/NHS-activated carboxy groups by a spontaneous hydrolysis. The incomplete regeneration of carboxy groups in pCB was accompanied by an excess of surface positive charge promoting the fouling from blood plasma. It was demonstrated that only the covalent coupling of amino acid agents such as glycine to active NHS-esters in the brush substantially improved resistance of BRE-functionalized pCB coatings to plasma fouling. We demonstrated that the BRE-functionalized and glycine-deactivated pHPMAA-CBMAA coatings with an optimized CBMAA molar content (15%) provided BRE capacity and resistance to plasma fouling that were comparable with the state-of-art ultralow-fouling carboxy-functional homopolymer coatings. In addition, their resistance to plasma fouling was shown to be better than that of pCBMAA coatings and much better than that of conventional OEG-SAMs.

The pHPMAA-CBMAA(15%) coatings functionalized with DNA-ON probes with high surface concentration (~1.4×10^{13} probes/cm^2) and glycine-deactivated exhibited fouling resistance to blood plasma that was two orders of magnitude better when compared to commonly used DNA ON-functionalized mixed OEG-SAMs. We believe that these findings will benefit future design and functionalization of carboxy-functional ultralow-fouling biorecognition coatings for effective biosensing in biological fluids.

Supporting Information

Supporting Information Available: synthesis of monomers, procedures of preparation and functionalization of polymer- and SAM-based coatings, SPR measurements details. This material is available free of charge via the Internet at http://pubs.acs.org.

AUTHOR INFORMATION

Corresponding Authors

* Prof. Jiří Homola, Ph.D., DSc., Institute of Photonics and Electronics, Czech Academy of Sciences, Chaberská 57, 18251 Prague, Czech Republic; Tel.: +420 266773404, E-mail: homola@ufe.cz

Author Contributions

The manuscript was written through contributions of all authors. / All authors have given approval to the final version of the manuscript.

ACKNOWLEDGMENT

This research was supported by the Czech Science Foundation (contract # P205/12/G118 and 15-09368Y), by the Ministry of Education, Youth and Sports of CR within the National

Sustainability Program II (Project BIOCEV-FAR LQ1604), by the project "BIOCEV" (CZ.1.05/1.1.00/02.0109), and by Praemium Academiae of the Academy of Sciences of the Czech Republic. Hana Lísalová and Eduard Brynda equally contributed to this work.

REFERENCES

(1) Murugaiyan, S. B.; Ramasamy, R.; Gopal, N.; Kuzhandaivelu, V. *Adv. Biomed. Res.* **2014**, 3, 67.

(2) Vo-Dinh, T.; Fales, A. M.; Griffin, G. D.; Khoury, C. G.; Liu, Y.; Ngo, H.; Norton, S. J.; Register, J. K.; Wang, H. N.; Yuan, H. *Nanoscale* **2013**, 5, 10127-10140.

(3) Homola, J. *Chem. Rev.* **2008**, 108, 462-493.

(4) Blaszykowski, C.; Sheikh, S.; Thompson, M. *Biomater. Sci.* **2015**, 3, 1335-1370.

(5) Vaisocherova, H.; Brynda, E.; Homola, J. *Anal. Bioanal. Chem.* **2015**, 407, 3927-3953.

(6) Pereira, A. D.; Rodriguez-Emmenegger, C.; Surman, F.; Riedel, T.; Alles, A. B.; Brynda, E. *Rsc Adv.* **2014**, 4, 2318-2321.

(7) Springer, T.; Bockova, M.; Homola, J. *Anal. Chem.* **2013**, 85, 5637-5640.

(8) Vaisocherová, H.; Ševců, V.; Adam, P.; Špačková, B.; Hegnerová, K.; Pereira, A. D.; Rodriguez-Emmenegger, C.; Riedel, T.; Houska, M.; Brynda, E.; Homola, J. *Biosens. Bioelectron.* **2014**, 51, 150-157.

(9) Rodriguez-Emmenegger, C.; Brynda, E.; Riedel, T.; Houska, M.; Subr, V.; Alles, A. B.; Hasan, E.; Gautrot, J. E.; Huck, W. T. *Macromol. Rapid Commun.* **2011**, 32, 952-957.

(10) Banerjee, I.; Pangule, R. C.; Kane, R. S. *Adv. Mater.* **2011**, 23, 690-718.

(11) Ladd, J.; Zhang, Z.; Chen, S.; Hower, J. C.; Jiang, S. *Biomacromolecules* **2008**, 9, 1357-1361.

(12) Yang, W.; Chen, S.; Cheng, G.; Vaisocherová, H.; Xue, H.; Li, W.; Zhang, J.; Jiang, S. *Langmuir* **2008**, 24, 9211-9214.

(13) Wang, J.; Yuan, S.; Zhang, Y.; Wu, W.; Hu, Y.; Jiang, X. *Biomater. Sci.* **2016**, 4, 1351-1360.

(14) Wang, Z.; Ma, G.; Zhang, J.; Yuan, Z.; Wang, L.; Bernards, M.; Chen, S. *Biomaterials* **2015**, 62, 116-127.

(15) Sun, F.; Hung H-Ch; Sinclair A.; Zhang P.; Bai T.; Galvan D. D.; Jain P.; Li B.; Jiang S.; Yu Q., *Nat. Commun.* **2016**, 7, 13437.

(16) Vaisocherová, H.; Yang, W.; Zhang, Z.; Cao, Z.; Cheng, G.; Piliarik, M.; Homola, J.; Jiang, S. *Anal. Chem.* **2008**, 80, 7894-7901.

(17) Lofas, S.; Johnsson, B.; Edstrom, A.; Hansson, A.; Lindquist, G.; Hillgren, R. M. M.; Stigh, L. **1995**, 10, 813-822.

(18) Lahiri, J.; Isaacs, L.; Tien, J.; Whitesides, G. M. *Anal. Chem.* **1999**, 71, 777-790.

(19) Brault, N. D.; Gao, C.; Xue, H.; Piliarik, M.; Homola, J.; Jiang, S.; Yu, Q. *Biosens. Bioelectron.* **2010**, 25, 2276-2282.

(20) Riedel, T.; Surman, F.; Hageneder, S.; Pop-Georgievski, O.; Noehammer, C.; Hofner, M.; Brynda, E.; Rodriguez-Emmenegger, C.; Dostálek, J. *Biosens. Bioelectron.* **2016**, 85, 272-279.

(21) Nakajima, N.; Ikada, Y. *Bioconjugate Chem.* **1995**, 6, 123-130.

(22) Sam, S.; Touahir, L.; Salvador Andresa, J.; Allongue, P.; Chazalviel, J.-N.; Gouget-Laemmel, A.; Henry de Villeneuve, C.; Moraillon, A.; Ozanam, F.; Gabouze, N. *Langmuir* **2009**, 26, 809-814.

(23) Palazon, F.; Montenegro Benavides, C.; Léonard, D.; Souteyrand, E. l.; Chevolot, Y.; Cloarec, J.-P. *Langmuir* **2014**, 30, 4545-4550.

(24) Wang, C.; Yan, Q.; Liu, H.-B.; Zhou, X.-H.; Xiao, S.-J. *Langmuir* **2011**, 27, 12058-12068.

(25) Booth, M. A.; Kannappan, K.; Hosseini, A.; Partridge, A. *Langmuir* **2015**, 31, 8033-8041.

(26) Lim, C. Y.; Owens, N. A.; Wampler, R. D.; Ying, Y.; Granger, J. H.; Porter, M. D.; Takahashi, M.; Shimazu, K. *Langmuir* **2014**, 30, 12868-12878.

(27) Brault, N. D.; White, A. D.; Taylor, A. D.; Yu, Q.; Jiang, S. *Anal. Chem.* **2013**, 85, 1447-1453.

(28) Vaisocherová-Lisalová, H.; Surman, F.; Víšová, I.; Vala, M.; Špringer, T.; Ermini, M. L.; Šípová, H.; Šedivák, P.; Houska, M.; Riedel, T.; Pop-Georgievski, O.; Brynda, E.; Homola, J. *Anal. Chem.* **2016**, 88, 10533-10539.

(29) Ikeda, S.; Kong, S. W.; Lu, J.; Bisping, E.; Zhang, H.; Allen, P. D.; Golub, T. R.; Pieske, B.; Pu, W. T. *Physiol. Genomics* **2007**, 31, 367-373.

(30) Iorio, M. V.; Ferracin, M.; Liu, C. G.; Veronese, A.; Spizzo, R.; Sabbioni, S.; Magri, E.; Pedriali, M.; Fabbri, M.; Campiglio, M.; Menard, S.; Palazzo, J. P.; Rosenberg, A.; Musiani, P.; Volinia, S.; Nenci, I.; Calin, G. A.; Querzoli, P.; Negrini, M.; Croce, C. M. *Cancer Res.* **2005**, 65, 7065-7070.

(31) Wang, K.; Zhang, S. L.; Marzolf, B.; Troisch, P.; Brightman, A.; Hu, Z. Y.; Hood, L. E.; Galas, D. J. *Proc Natl Acad Sci U. S. A.* **2009**, 106, 4402-4407.

(32) Jones, D. M.; Brown, A. A.; Huck, W. T. S. *Langmuir* **2002**, 18, 1265-1269.

(33) Rodriguez-Emmenegger, C.; Houska, M.; Alles, A. B.; Brynda, E. *Macromol. Biosci.* **2012**, 12, 1413-1422.

(34) Ulbrich, K.; Šubr, V.; Strohalm, J.; Plocová, D.; Jelínková, M.; Říhová, B. *J. Controlled Release* **2000**, 64, 63-79.

(35) Springer, T.; Piliarik, M.; Homola, J. *Sens. Actuators, B* **2010**, 145, 588-591.

(36) Pereira, A.D.; Rodriguez-Emmenegger, C.; Surman, F.; Riedel, T.; Alles, A. B.; Brynda, E. *Rsc Adv.* **2014**, 4, 2318-2321.

(37) Šípová, H.; Homola, J. *Anal. Chim. Acta* **2013**, 773, 9-23.

(38) Avino, A.; Huertas, C. S.; Lechuga, L. M.; Eritja, R. *Anal. Bioanal. Chem.* **2016**, 408, 885-893.

Table of Contents (TOC) Figure: